ASTEROIDAL SPACE WEATHERING: THE MAJOR ROLE OF FeS.

L. P. Keller[1], Z. Rahman[2], T. Hiroi[3], S. Sasaki[4], S. K. Noble[5], F. Hörz[1] and M. J. Cintala[1] [1]ARES, NASA/JSC, Houston, TX 77058, [2]Jacobs ESCG, NASA/JSC, Houston, TX 77058, [3]Dept. Geological Sciences, Brown Univ., Providence, RI 02912, [4]RISE Project, National Astronomical Observatory of Japan, 2-12, Hoshigaoka-cho, Mizusawa-ku, Oshu, Iwate 023-0861, Japan. [5]NASA GSFC Mail Code 691, Greenbelt, MD 20771, (Lindsay.P.Keller@nasa.gov).

Introduction. Space weathering (SW) effects on the lunar surface are reasonably well-understood from sample analyses [1-3], remote-sensing data, and experiments [e.g. 2, 4, 5], yet our knowledge of asteroidal SW effects are far less constrained. While the same SW processes are operating on asteroids and the Moon, namely solar wind irradiation, impact vaporization and condensation, and impact melting, their relative rates and efficiencies are poorly known, as are their effects on such vastly different parent materials. Asteroidal SW models based on remote-sensing data and experiments are in wide disagreement over the dominant mechanisms involved and their kinetics [e.g. 6, 7]. Lunar space weathering effects observed in UV-VIS-NIR spectra result from surface- and volume-correlated nanophase Fe metal (npFe^0) particles. In the lunar case, it is the tiny vapor-deposited npFe^0 that provides much of the spectral reddening, while the coarser (largely melt–derived) npFe^0 produce lowered albedos [8, 9]. Nanophase FeS (npFeS) particles are expected to modify reflectance spectra in much the same way as npFe^0 particles. Here we report the results of experiments designed to explore the efficiency of npFeS production via the main space weathering processes operating in the asteroid belt.

Vaporization/Condensation Experiments. We previously reported the results of simulated micrometeorite impact into chondritic targets using a pulsed laser technique [10]. These experiments showed the formation of surface melts on the targets and the formation of abundant nanophase Fe particles in the melt layer. In these experiments, a glass slide was placed ~1 cm above the meteorite target in order to collect part of the vapor plume generated by the repeated laser impacts [11]. We used a focused ion beam (FIB) instrument to extract a thin section through the vapor-deposited coating that was generated from the Ehole H5 chondrite and analyzed the section in the transmission electron microscope (TEM). The 50-nm thick coating consists of amorphous Mg-rich silicate glass and abundant nanophase (2-5 nm) FeS (npFeS) particles. The coating is stratified with a non-uniform distribution of npFeS particles (Fig. 1). Relative to the bulk composition of Ehole, the vapor-deposited coating is depleted in Mg, enriched in Fe and strongly enriched in S by a factor of ~10. The Fe (sulfide)/Fe (metal) ratio in bulk Ehole is 0.2 [12] while that in the vapor coating is ~9. Essentially all of the Fe in the vapor-deposited coating is present as npFeS. The uppermost surface of the vapor-deposited coating shows numerous sub-µm Mg-silicate melt spherules.

Irradiation/Sputtering Experiments. Laboratory experiments were used to explore the mechanism of S depletions observed at Eros [13]. Irradiation of FeS with 4 keV He+ results in preferential sputtering of S and the formation of a thin 2-3 nm, compact Fe metal layer that armors the surface [14]. The zone of S loss extends to a depth of ~8-10 nm below the exposed surface. Despite this S loss, the FeS retains its crystallinity and shows no sign of incipient amorphization. Irradiation of FeS with 5kV Ga+ resulted in preferential sputtering of S and the formation of a 5-8-nm thick surface layer of nanophase Fe metal. X-ray mapping shows that the zone of S sputtering extends to a depth of nearly 20 nm, but there is no evidence for FeS amorphization, consistent with our previous work [15].

The irradiation experiments also show that the relative sputtering rate of FeS is much higher than olivine or enstatite. Sputtering experiments utilizing 30 kV and 5 kV Ga ions in the FIB produced pits in troilite that were ~4X deeper than the adjacent pits in enstatite or forsterite (Fig. 2). The sputter yield under these conditions is such that for every Si atom sputtered from enstatite, ~14 S atoms are sputtered from FeS. We have performed similar sputtering experiments on Fe-bearing niningerite (MgS) and co-existing enstatite from the ALH 84170 EH3 chondrite. MgS also sputters more rapidly than enstatite with a relative Si:S sputter yield of 1:8. For MgS, sulfur is highly depleted at the surface and the S-depletion zone extends to a depth of ~15 nm (using 5 kV Ga+). There is a corresponding zone of Mg and especially Fe enrichment that extends from 5 to ~10 nm below the surface, respectively.

Shock Experiments. Hörz et al. [16] showed that iron metal and FeS are readily mobilized by shock. They performed shock-recovery experiments on comminuted powders of ALH 85017, a L6 ordinary chondrite. At shock pressures of 67 GPa (corresponding to an impact velocity of ~5 km/s, near the asteroidal mean value of 5.3 km/s [17]) ~50% of the target material was molten. The FeS and Fe metal formed immiscible melts that are distributed throughout the silicate melt-glass as sub-µm particles [16]. We used the scanning electron microscope to examine samples shocked to 50 GPa and observed schlieren dominated by npFeS

particles in feldspathic-melt glass (Fig. 3). FIB/TEM analyses of these shock melts are underway to determine the nature and size-frequency distribution of the nanophase inclusions.

Conclusions. Fe-sulfide, a major mineralogical constituent of ordinary and carbonaceous chondrite meteorites, is readily vaporized by simulated micrometeorite impacts. The vaporized material recondenses as npFeS similar in size range to the $npFe^0$ in lunar samples that is responsible for the reddened slopes in VIS-NIR reflectance spectra. Ion irradiation of FeS results in preferential sputtering of S and produces nanophase Fe metal as a by-product. Shock experiments simulating asteroidal impact velocities show that FeS and Fe metal are readily mobilized and incorporated as nanophase inclusions in shock melts. Taken together, these results suggest that npFeS plays a major role in asteroidal space weathering.

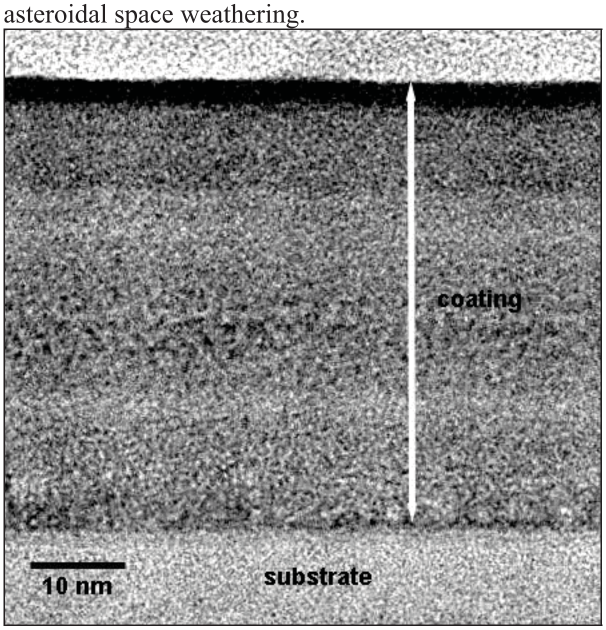

Figure 1. Brightfield TEM image of the 50-nm thick-vapor-deposit obtained by laser irradiation of the Ehole H5 chondrite. Dark specks are npFeS particles.

References. [1] Keller, L. P. and McKay, D. S. (1997) *GCA*, 61, 2331. [2] Pieters, C. M. et al. (2000) MAPS, 35, 1101. [3] Noble, S. K. *et al*. (2012) *LPSC* 43, #1239. [4] Noble, S. K. *et al.* (2001) *MAPS* 36, 31. 148. [5] Christoffersen, R. *et al*. (2012) *MAPS* 47, #5341. [4] Keller, L. P. et al. (2010) LPS XXXXI, #1172. [5] Christoffersen, R. et al. (2011) MAPS, in press. [6] Vernazza, P. *et al*. (2009) *Nature* 458, 993. [7] Willman, M. *et al*. (2010) *Icarus* 208, 758. [8] Keller, L. P. *et al.* (1998) New Views of the Moon, *LPI Contribution* 958, 44. [9] Noble, S. K. *et al*. (2007) *Icarus* 192, 629. [10] Noble, S. K. et al. (2011) *LPSC* XLII, #1382. [11] Yamada, M. *et al*. (1999) *Earth Planets Space* 51, 1255. [12] Jarosewich, E. (1990) *Meteoritics* 25, 323. [13] Loeffler, M. *et al*. (2008) *Icarus* 195, 622. [14] Keller, L. P. and Rahman, Z. (2011) *MAPS* 46, #5455. [15] Christoffersen, R. *et al*. (2011) *MAPS* 46, 950 [16] Hörz, F. *et al*. (2005) *MAPS* 40, 1329. [17] Bottke, W., *et al.* (1994), *Icarus* 107, 255.

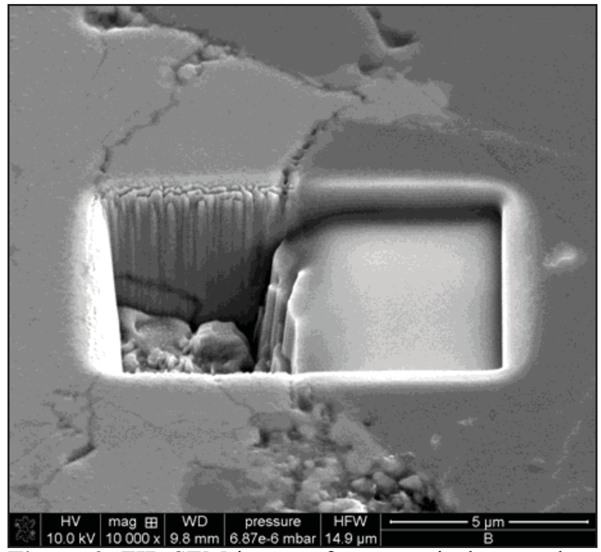

Figure 2. FIB-SEM image of sputter pit that overlaps a troilite- enstatite grain boundary. The pit depth ratio is ~4 showing that troilite sputters more easily than enstatite.

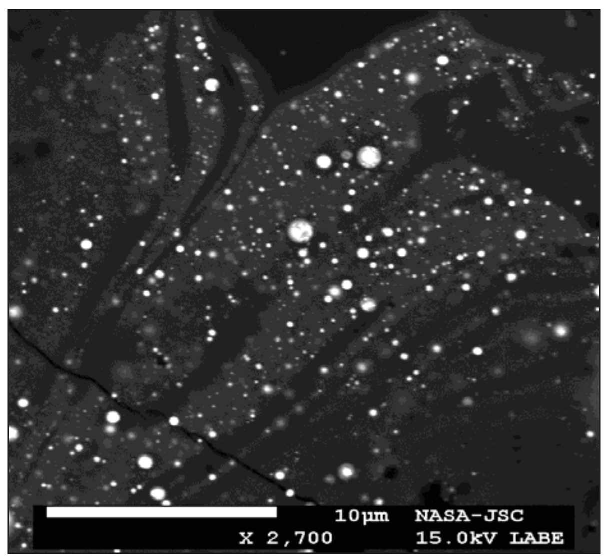

Figure 3. Backscattered SEM image of impact melt with abundant nanophase FeS and Fe^0 inclusions produced at a maximum shock pressure of 50 GPa into a comminuted ALH 85017 target.

Acknowledgements. This work supported by a NASA Cosmochemistry Program grant to LPK.